Key Points:

- Current sounders' sub-footprints exhibit high moisture spatial variations over land, especially in the pre-convection environment
- Current sounders have limited capability to capture small-scale moisture spatial variation, while future GEO sounders have such capability
- A higher spatial resolution sounder provides more footprints with clear sky measurements for application such as radiance assimilation

Can Current Hyperspectral Infrared Sounders Capture the Small Scale Atmospheric Water Vapor Spatial Variations?

Di Di[1,2] ⓘ, Jun Li[3] ⓘ, Zhenglong Li[3] ⓘ, Jinlong Li[3] ⓘ, Timothy J. Schmit[4] ⓘ, and W. Paul Menzel[3] ⓘ

[1]Collaborative Innovation Center on Forecast and Evaluation of Meteorological Disasters, Nanjing University of Information Science and Technology, Nanjing, China, [2]Key Laboratory for Aerosol-Cloud-Precipitation, China Meteorological Administration, School of Atmospheric Physics, Nanjing University of Information Science and Technology, Nanjing, China, [3]Cooperative Institute for Meteorological Satellite Studies, University of Wisconsin – Madison, Madison, WI, USA, [4]Advanced Satellite Products Branch, STAR/NESDIS/NOAA, Madison, WI, USA

Abstract Severe storms are often associated with high temporal and spatial variations in atmospheric moisture deviation. Satellite-based hyperspectral IR sounders are widely used for weather forecasting and data assimilation in numerical weather prediction. Current infrared (IR) sounders have spatial resolutions ranging from 12 to 16 km, with future sounders improved to 4–8 km. It is important to understand if measurements from the current and future IR sounders can capture small-scale atmospheric moisture variations, especially during mesoscale weather events. Using measurements from three Advanced Himawari Imager moisture absorption bands, different sounder resolutions are simulated for sub-footprint moisture variation analysis. Current sounders are limited when attempting to capture small-scale moisture variations, especially over land and in the pre-convection environment. In contrast, future sounders such as the InfraRed Sounder with 4 km resolution can better capture such small-scale variations. In addition, the higher spatial resolution IR sounders provide more clear sky observations for applications.

Plain Language Summary Measurements from satellite-based hyperspectral infrared (IR) sounders have been widely used in numerical weather prediction (NWP), nowcasting, and climate applications. Most IR sounder data used by NWP are over the ocean and in clear skies, especially for water vapor absorption channels. To better understand the causes of limited water vapor absorption IR radiance assimilation over land, the sub-footprint moisture variations under different hyperspectral IR sounder spatial resolutions are analyzed using three water vapor absorption bands radiances from the Advanced Himawari Imager. The current hyperspectral IR sounders with spatial resolutions from 12 to 16 km have a limited ability to capture small-scale water vapor variations, especially over land and in the pre-convection environment, while future geostationary IR sounders such as the InfraRed Sounder onboard the Meteosat Third Generation can capture small-scale moisture variations, helping to meet requirements for regional applications such as data assimilation and nowcasting.

1. Introduction

Severe storms often occur when the atmospheric moisture exhibits high temporal and/or spatial variations (e.g., a cold front or dryline; Atkins et al., 1998). Measurements of water vapor vertical distributions as well as temporal and spatial variations are very important for nowcasting and forecasting such high-impact weather events (Li et al., 2011, 2012). The measurements are also critically important for improving numerical weather prediction (NWP) models through data assimilation. Today's hyperspectral infrared sounders such as the Atmospheric Infrared Sounder (AIRS), Infrared Atmospheric Sounder Interferometer (IASI), Hyperspectral Infrared Atmospheric Sounder (HIRAS), and Cross-track Infrared Sounder (CrIS; Menzel et al., 2018), have been widely used for measuring the vertical distributions of atmospheric temperature and moisture, and measurements from those sounders are operationally assimilated into NWP models for improving regional and global weather forecasts. Recently, hyperspectral IR sounders are being developed for measuring atmospheric temperature and water vapor profiles with a high temporal resolution, which

can provide both thermodynamic and dynamic information for various applications. For example, using measurements from the Geosynchronous Interferometric Infrared Sounder (GIIRS), the first geostationary hyperspectral IR sounder (Yang et al., 2017), Yin et al. (2021) have demonstrated that higher temporal resolution provides better impact on tropical cyclone forecasts with a 4DVAR assimilation system in a global NWP model; Ma et al. (2021) developed novel methodologies for extracting 4D horizontal wind fields from high temporal GIIRS water vapor radiances under clear skies and some cloudy situations, and demonstrated that higher temporal resolution (e.g., 15 min vs. 30 min) provides better 4D wind retrievals.

Spectral resolution and coverage, along with signal-to-noise ratio play an important role in obtaining high-quality information from measurements for applications (F. Wang et al., 2007). Temporal resolution is also very important for nowcasting applications. For example, Li et al. (2011) demonstrated that a geostationary hyperspectral IR sounder with high temporal resolution would provide more detailed stability information in the pre-convective environment, which is useful for identifying favorable locations for convective initiation. Y.-K. Lee et al. (2017) found that the 10 min interval Advanced Himawari Imager (AHI) water vapor absorption radiance measurements provide more detailed temporal variation information on the pre-landfall environment for Typhoon Nangka than 30 min and hourly interval data, showing the value of higher temporal resolution data.

However, the capability of those hyperspectral IR sounders with different spatial resolutions to capture small-scale (e.g., storm scale) atmospheric moisture spatial variations has not been well understood, except that higher spatial resolution will provide more clear observations (Menzel et al., 1984; Seemann et al., 2003; Smith et al., 1996) for various applications, especially data assimilation which will improve NWP-based forecasts. Small-scale (2–20 km) moisture features are important in understanding and predicting convective initiation (Henken et al., 2016), while mesoscale (10–1,000 km) moisture features are used for predicting high impact weather events such as fronts, squall lines, tropical cyclones etc (LeMone et al., 1998). It is important that hyperspectral IR sounders have the capability to capture both small-scale and mesoscale moisture features for various applications. The current hyperspectral IR sounders onboard the polar orbiting satellites have spatial resolutions between 12 and 14 km at nadir (e.g., IASI, AIRS, HIRAS, and CrIS). GIIRS on FengYun-4A launched in December 2016 has even coarser spatial resolution at 16 km while GIIRS on FengYun-4B launched in June 2021 has better spatial resolution at 12 km. Future GIIRS instruments will have a further improved resolution at 8 km while the future InfraRed Sounder (IRS) on the Meteosat Third Generation (MTG) satellites (Freudling et al., 2017; Schmetz et al., 2012) will have even higher spatial resolution at 4 km, as well as the planned US Geostationary Extended Observations (GeoXO) Sounder. To understand the value of higher spatial resolutions for capturing small-scale atmospheric water vapor spatial variations, and the implications on applications, it is important to address and understand the following scientific questions:

1. Can current and future hyperspectral IR sounders capture small-scale water vapor spatial variations, especially during mesoscale events?
2. How large is the sub-footprint moisture spatial variation for a given hyperspectral IR sounder resolution? Does the hyperspectral IR sounder sub-footprint moisture variation have seasonal, regional and diurnal characteristics?
3. What are the implications of sub-footprint moisture variations on the applications of the current hyperspectral IR sounder water vapor channel radiances for nowcasting and data assimilation in NWP models?
4. What is the required resolution for future hyperspectral IR sounders to depict small-scale water vapor variation for various applications?

In this study, radiance measurements from the AHI with 2 km spatial resolution are used to simulate various hyperspectral IR sounder resolutions, and the sub-footprint water vapor spatial variations under these resolutions are analyzed to address these questions. Section 2 describes the data used in this study. Section 3 provides methodologies and approaches. Section 4 provides the results and analysis, and the conclusions plus a discussion are given in Section 5.

2. Data and Methodologies

2.1. Data

The AHI (Bessho et al., 2016) onboard Himawari-8 satellite and the Advanced Baseline Imager (ABI; Kalluri et al., 2018; Schmit et al., 2005, 2017) onboard GOES-16/-17 satellites have similar spectral bands measuring weather systems with a very high spatial (0.5 km for 0.64 μm, 1 km for 0.47 and 0.86 μm, 2 km for other near IR and IR bands for AHI) and temporal resolutions (10 min for the full disk, 2.5 min for two specific regions for the AHI). Among the AHI spectral bands, there are three water vapor absorption bands centered at 6.3, 6.9, and 7.3 μm (bands 8, 9, and 10 respectively), with weighting function peaks around 350, 450, and 600 hPa, respectively, depending on the atmospheric state (Di et al., 2016). Together with the 12 μm weak water vapor absorption band, both AHI and ABI provide atmospheric layered precipitable water (LPW) and total precipitable water (TPW; Schmit et al., 2019) which are useful for weather nowcasting and forecasting applications. Radiances from the three water vapor bands have also been demonstrated to be useful for improving global and regional NWP forecasts (Honda et al., 2018; P. Wang et al., 2017; P. Wang, Li et al., 2018; Y. Wang, Liu, et al., 2018), especially when combined with appropriate cumulus and microphysical parameterization schemes (Lu et al., 2019).

Since the AHI has three water vapor bands with both high spatial and temporal resolutions, the data can be used to investigate and understand the impact of resolution on various applications. AHI radiance measurements along with cloud mask products from one year (2016) have been used. The key questions investigated relevant to the current hyperspectral IR sounders include: (a) How large are the sub-footprint water vapor variations? (b) How will those sub-footprint water vapor variations impact applications such as data assimilation? The data at four times (00 UTC, 06 UTC, 12 UTC, and 18 UTC) are used to simulate the radiances for various hyperspectral IR sounders with different spatial resolutions; in addition, seasonal and diurnal characteristics of the sounder's sub-footprint water vapor variations are investigated. AHI data with local zenith angles (LZA) greater than 65° are excluded from the analysis. Another option would have been to use Moderate Resolution Imaging Spectroradiometer (MODIS) radiance measurements which have the required global coverage; however, MODIS has only two water vapor absorption bands, and does not provide enough temporal measurements for studying diurnal characteristics.

2.2. Methodologies

Measurements from three AHI water vapor absorption bands with 2 km (nadir) resolution are used to simulate radiances from current hyperspectral IR sounders with different spatial resolutions (e.g., 12 km for IASI and GIIRS/FY4B, 14 km for AIRS/CrIS/HIRAS, 16 km for GIIRS/FY-4A) and from future hyperspectral IR sounders (e.g., 4 km for IRS, 8 km for future FY4 satellites). The following approach is used for the simulations:

1. For each AHI water vapor band, the 2 km radiances within the sounder footprint are averaged and converted to brightness temperature (BT) to represent the sounder water vapor BT (although for a broad spectral band), i.e., the average of 16 pixels from a 4 x 4 box represent the BT of an 8 km sounder. The term sub-footprint is specifically for IR sounders, while the term pixel is used for imagers (e.g., AHI). So each IR sub-footprint contains many AHI pixels with the 2 km spatial resolution. Since the spatial response function is not applied in the averaging for simplicity, there might be some errors in simulating the BTs for a given advanced IR sounder resolution; however, the error should be small (e.g., less than 0.1 K; Zhang et al., 2006). In addition, since the purpose is to study the relative change when the hyperspectral IR sounder spatial resolution varies, whether or not the spatial response function is applied will have little impact on the findings and conclusions

2. Detecting clear hyperspectral IR sounder sub-footprints is made possible by the collocated AHI 2 km cloud mask generated with the FengYun-4 science product algorithm (Min et al., 2017), the algorithm is reliable for generating accurate cloud mask products according to P. Wang, Li, et al. (2019) and X. Wang, Min, et al. (2019). There are four scene types for a given AHI pixel: confident clear, probably clear, confident cloudy, and probably cloudy. Since AHI has similar measurement characteristics as ABI, especially for the three water vapor absorption bands, the ABI and CrIS are used for demonstration purposes. Figure 1 shows an example of the ABI Band 8 BTs at 2 km resolution superimposed on CrIS footprints
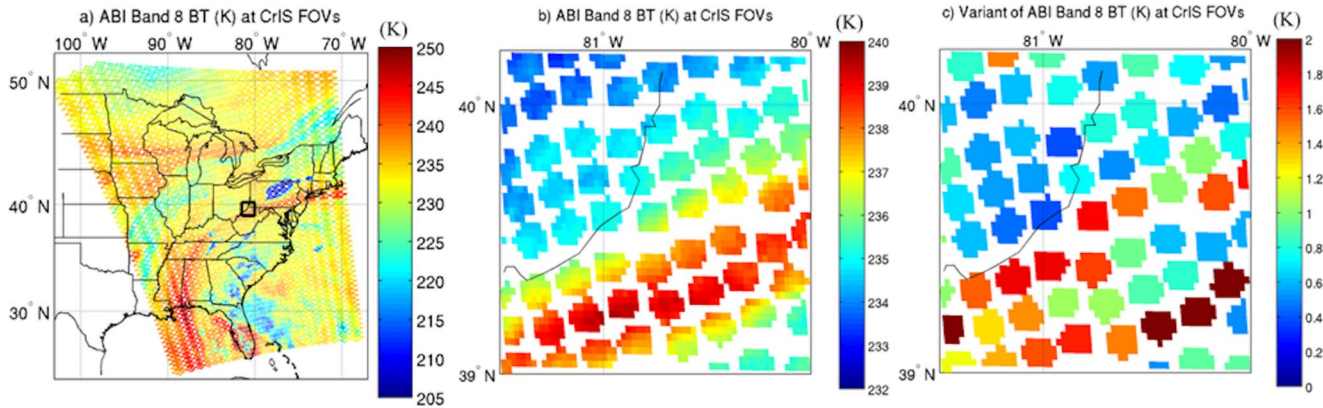
Figure 1. ABI Band 8 BTs at 2 km resolution superimposed on CrIS footprints for a CrIS granule (left panel) and the zoom-in of ABI band 8 BTs from a small clear sky area depicted in the black box in the left panel (middle panel), along with the CrIS sub-footprint BTVs (right panel) at 18:22 UTC on May 15, 2018.

(Nagle & Holz, 2009) for a CrIS granule (left panel) and zoomed in on the ABI Band 8 BTs from a small clear sky area depicted in the black box in the left panel (middle panel), along with the CrIS sub-footprint BT variations (BTVs, right panel) which are BT differences between coldest and warmest pixels within the footprint (see further explanation in (3) below) at 18:22 UTC on May 15, 2018

The clearness of an IR sounder footprint is defined by the percentage of confident clear and probably clear AHI pixels within the whole sub-footprint. For example, if all the AHI pixels within an IR sounder sub-footprint are confident clear or probably clear, this footprint is considered completely clear; if the percentage of the confident clear and probably clear AHI pixels within an IR sounder sub-footprint is greater than 25% (this ensures at least 1 AHI pixel within a sounder footprint), then this IR sounder sub-footprint is considered partly clear. With a collocated imager like MODIS and an advanced IR sounder like AIRS, IR sounder sub-footprint cloud characterization can be conducted (Li et al., 2004), and the partly clear footprint can be cloud-cleared (Li et al., 2005) to obtain clear equivalent radiances for better IR radiance assimilation in cloudy skies (Li et al., 2016, 2021; P. Wang et al., 2014, 2015; P. Wang, Li, et al., 2019; X. Wang, Min, et al., 2019). As long as the imager and sounder are on the same platform, the imager can help the sounder data application, and vice versa.

3. IR sounder sub-footprint BTV is calculated for three AHI water vapor absorption spectral bands. Only completely clear footprints are used to characterize the BTV. For each hyperspectral IR sounder, the BTV is computed for each of the three AHI water vapor bands, and it is then used to analyze the sub-footprint atmospheric moisture spatial variations for the given IR sounder footprint spatial resolutions. The sub-footprint BTV is defined as

$$BTV = BTmax - BTmin \qquad (1)$$

BTmax and BTmin are the BT of warmest and coldest AHI pixels, respectively, within the IR sounder sub-footprint. Larger BTV indicates larger sub-footprint moisture variation while a smaller BTV means smaller sub-footprint moisture variation. The actual BTV could be larger than that calculated from Equation 1 using AHI due to the limitation of AHI's 2 km resolution.

The spatial variations in radiances or BT measurements from AHI water vapor absorption bands can be interpreted as changes in moisture averaged from different atmospheric layers, which are nearly proportional to the natural logarithm of the humidity changes. This radiance-humidity relationship has been illustrated in many studies (Iacono et al., 2003; Soden & Bretherton, 1993; Xue et al., 2020), which found that this simple radiance-humidity relationship explains greater than 90% of the variances in BT for water vapor bands. For Band 8 (centered at 6.28 μm), a 2 K decrease in BT corresponds to a water vapor increase of ∼30% (∼40%) around 350 hPa for a summer (winter) profile. And for Band 9 and Band 10 (centered at 6.9 and
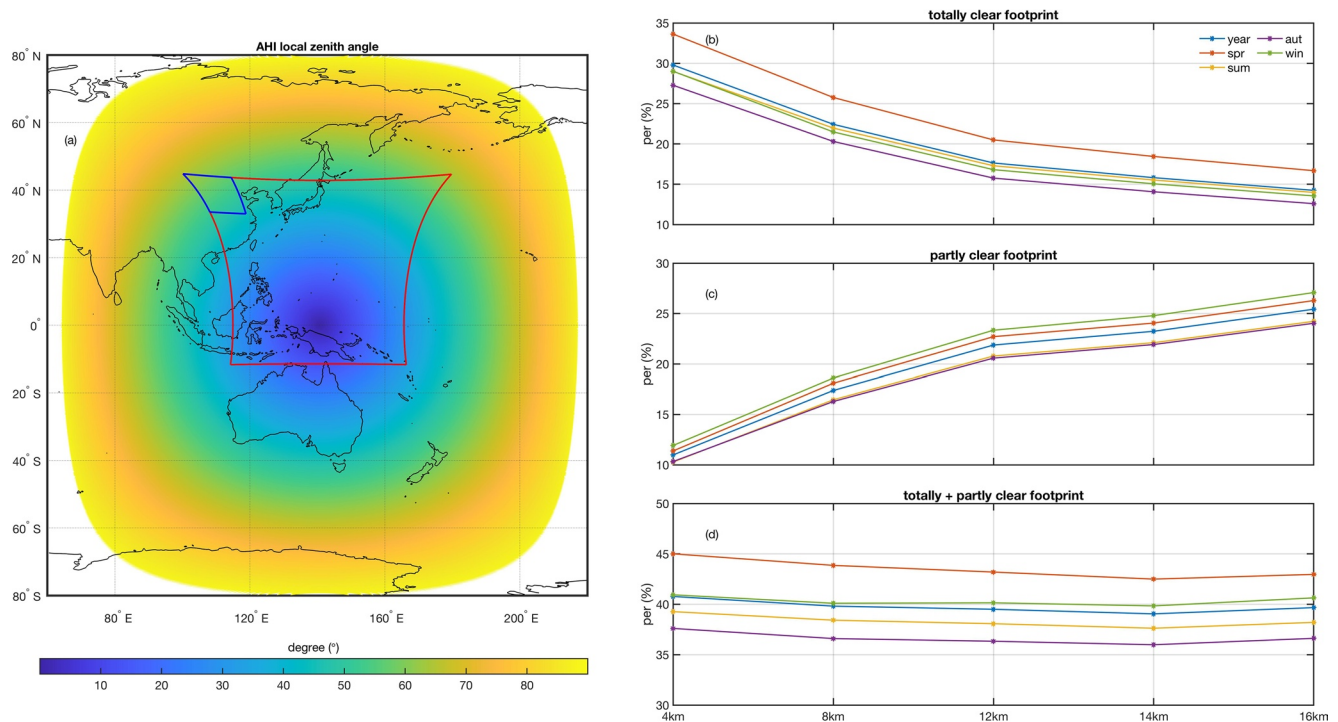
Figure 2. The selected study region (the red frame) overlaying a LZA image, along with a smaller north China region (the blue frame) to represent specific coverage over land (left panel), plus the percentages of totally clear footprints, partly clear footprints, and totally clear plus partly clear footprints over the study region, for different seasons of 2016 as well as the whole year (right panels).

7.3 µm, respectively), the same BTV represents slightly larger water vapor changes around 450 and 600 hPa, respectively.

Significant moisture variations (larger than 5 K) within the small region (middle panel, Figure 1) are observed. In addition, the CrIS sub-footprint moisture spatial variation can reach between 1 and 2.0 K (equivalent to ∼15%–30% variation in moisture) for BTV in this particular case (right panel). Such strong sub-footprint spatial variations, without being accounted for, may introduce additional uncertainties in the quantitative applications of CrIS radiances, i.e., radiance assimilation or sounding retrievals.

3. Results and Analysis

To minimize the influence of LZA (e.g., greater than 65°) and to facilitate the construction of various IR sounder spatial resolutions, a subset study region is selected. Figure 2 shows this study region (marked by the red frame) overlaying a LZA image, along with a smaller northern region (marked by the blue frame) to represent specific coverage over land; the right panels show the percentages of totally clear footprints, partly clear footprints, and totally clear plus partly clear footprints over the study region, for different seasons.

From Figure 2, it can be seen that:

1. There are significant changes in the percentage of clear footprints when the spatial resolution decreases from 4 km (∼30%) to 12 km (∼17%) in the annual average, while the percentage of clear footprints changes slowly when the resolution further decreases from 12 km (∼17%) to 16 km (∼14%), indicating that an IR sounder spatial resolution better than 12 km is very helpful to increase the clear footprint coverage for applications such as sounding retrieval and radiance assimilation in NWP
2. The clear percentage has seasonal differences. A hyperspectral IR sounder has more clear observations in spring while fewer clear observations in fall over our study region. In addition, no obvious clear percentage diurnal differences are observed (results are shown in Figure S1). According to previous findings (King et al., 2013), the occurrence of cirrus or convection clouds corresponds to the intertropical convergence zone whose location has seasonal movement in latitude. And the occurrence of altocumulus and

altostratus is highly relevant to frontal cyclones, which are directly influenced by the Asian monsoon. These might partly explain the seasonal variation of clear or cloud observations. Of course, the seasonal differences are dependent on the region

3. If the advanced IR sounder spatial resolution is increased from the current 12–16 km (IASI, GIIRS/FY4B, CrIS, AIRS, HIRAS, GIIRS/FY4A) to 8 km (e.g., future GIIRS), the percentage of clear footprints could increase from ∼17% to ∼23% over this region; with the required signal-to-noise ratio, this improvement could significantly increase the clear data coverage for assimilation into NWP models, especially regional NWP models. Considering that the MTG IRS will have 4 km resolution, the percentage of clear data coverage could be around 30% according to this study, which is very useful for deriving high temporal resolution preconvention atmospheric instability information (Li et al., 2011, 2012) for local severe storm nowcasting and global/regional NWP assimilation for weather forecasting. In addition, this higher resolution could better capture the spatial moisture gradient which is critical for nowcasting. This analysis is consistent with that of Seemann et al. (2003), which showed that a finer spatial resolution for an IR sounder can not only increase the coverage of water vapor retrieval products, but also increase the capability of depicting moisture spatial gradients

4. Contrary to the clear observations, the percentage of partly clear footprints increases when spatial resolution decreases, which leads to the combined percentage of clear and partial clear footprints not changing substantially. The current sounders (12–16 km) have more than 20% partly clear footprints, which could be used in DA after cloud-clearing (Li et al., 2005) using collocated sub-footprint imager clear radiance observations if the imager and the sounder are on the same platform. That has been demonstrated by MODIS/AIRS (P. Wang et al., 2015), and VIIRS/CrIS (P. Wang et al., 2017), where imager-based sounder cloud-cleared radiances further improve hurricane forecasts when used together with clear sounder radiances (radiances from clear footprints and channels not affected by clouds). It is particularly important to apply a cloud-clearing technique to sounders such as GIIRS/FY4A with coarser spatial resolution (16 km) for obtaining more data for assimilation applications (Li et al., 2016) because of the large percentage of partly clear footprints (∼25%)

The relatively small improvement in obtaining clear footprints for the relatively large decrease in spatial resolution is due to the fact that the density of footprints (number of footprints for given size of area) was held the same and the statistic is not computed for a given Field of Regard (FOR) size (i.e., the area resolution desired for the final radiance spectra to be assimilated, each CrIS FOR contains 9 footprints, and one IASI FOR contains 4 footprints). If the density of footprints was allowed to increase for a given FOR size, by decreasing the footprint size as would be the case in using detector arrays, then the percentage of clear footprints for a given FOR size would improve dramatically.

Figure 3 shows annual averaged sub-footprint BTV images for different spatial resolutions (top panels) for AHI Band 8 (6.28 μm band) along with the probability distribution of sub-footprint BTVs (lower left/middle panel), and the annual averaged BTVs for three regions including ocean, land and the northern land region (lower right panel). It can be seen that:

1. From the sub-footprint BTV imagery, spatial variations show geographic dependency; they are larger over land than over ocean; in addition, they are larger over the land in the north than in the south, which might be partly due to large LZA over the region in this analysis. It is also very clear that finer spatial resolution corresponds to smaller sub-footprint BTVs. Finer spatial resolution also leads to less spatial variation within a IR sounder's footprint; capturing water vapor spatial variation, that is, along the front or dry lines, is critically important

2. From the probability distributions, most clear data (more than 97%) have sub-footprint BTVs less than 0.5 K when the resolution reaches 4 km; when the resolution is degraded to 8 km, 80% of the clear data still have BTVs less than 0.5 K. However, when the resolution is further degraded to 12–16 km, the clear data with sub-footprint BTV less than 0.5 K are significantly reduced (e.g., about 55% for 12 km, 45% for 14 km and 35% for 16 km). For all the resolutions, about 80% of the data have BTVs less than 1.0 K and about 95% of the data have BTVs less than 1.5 K. There is still a small portion (2%–5%) of the data with BTVs greater than 1.5 K from current IR sounders with a spatial resolution between 12 and 16 km. Ideally, the sub-footprint BTV should be smaller or comparable to the combined uncertainties from the observation and radiative transfer model for quantitative applications. Finer spatial resolutions for
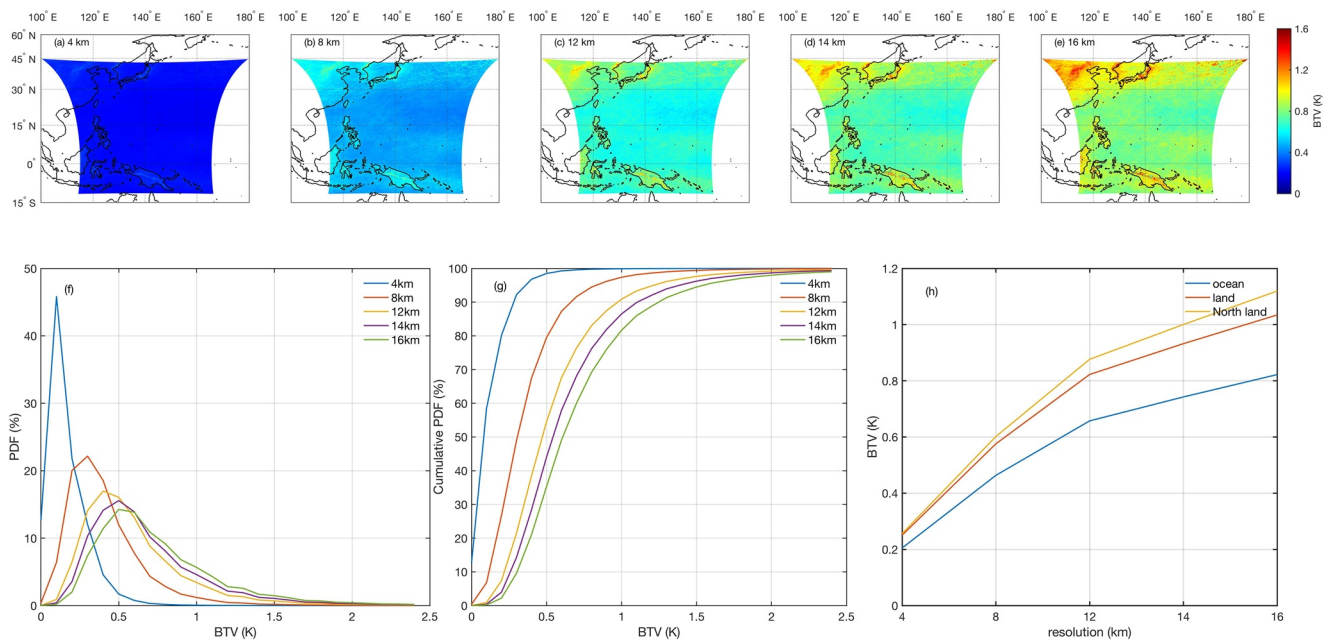
Figure 3. Annual averaged sub-footprint BTV images for spatial resolutions between 4 and 16 km (top row) for AHI Band 8 (6.28 μm band) along with the probability distribution and the cumulative probability distribution of sub-footprint BTV (lower left/middle panel), and the annual averaged BTVs for three regions including ocean, land and the northern land region (lower right panel).

IR sounders may significantly reduce the complications caused by sub-footprint BTVs. Figure 3 may indicate that the ability in capturing the small-scale variations would be linearly improved with finer resolutions. However, in reality, such ability might saturate when the signals of the small-scale variations are smaller than the observation uncertainties. Further improvement in resolution might provide further value on small-scale moisture variation if the observations errors are less than the needed signals for such variations

3. The statistics on sub-footprint BTVs show that upper tropospheric moisture (Band 8) has a slightly larger sub-footprint BTV than the middle-low tropospheric moisture (shown in the Supplemental File). This means that the upper troposphere moisture has more spatial variations as a percentage change than that of the middle-low troposphere. But in terms of mixing ratio, that is not necessarily true. The sub-footprint BTVs over land are obviously larger than those over the ocean. Over land, moisture over the north has further larger sub-footprint BTVs than over the south in this study region. In addition, sub-footprint BTVs have slight seasonal differences but no noticeable diurnal differences (See Figure S3)

For 4 km sounders, the average sub-footprint BTV is around 0.3 K for all three bands. However, when the spatial resolution is degraded to 8 km, the average sub-footprint BTV is larger than 0.5 K over land, and the current sounders with spatial resolutions between 12 and 16 km have typical average sub-footprint BTVs between 0.8 and 1.5 K over land. As mentioned, a 1 K variation in Band 8 corresponds to a 10%−20% moisture variation depending on the atmospheric humidity. Again, such sub-footprint BTVs, without being accounted for, may introduce additional uncertainties in quantitative applications such as radiance assimilation and sounding retrievals.

4. A Local Severe Storm Event Analysis

By assuming an IR sounder with 16 km resolution, Figure 4 shows BTV at 13:00 local time from three AHI water vapor bands (left panels) along with BT images (middle panels), and the BT images at 19:00 local time (right panels). It can be seen that at 13:00 local time, there are significant spatial variations in the clear sub-footprint BTVs, and the BT imagery also shows substantial moisture variations from all three bands over that region. And the spatial variations in BTVs for three bands are not completely the same. On the whole, the BTV spatial patterns are closer between band 8 and band 9, both of which detect water vapor at
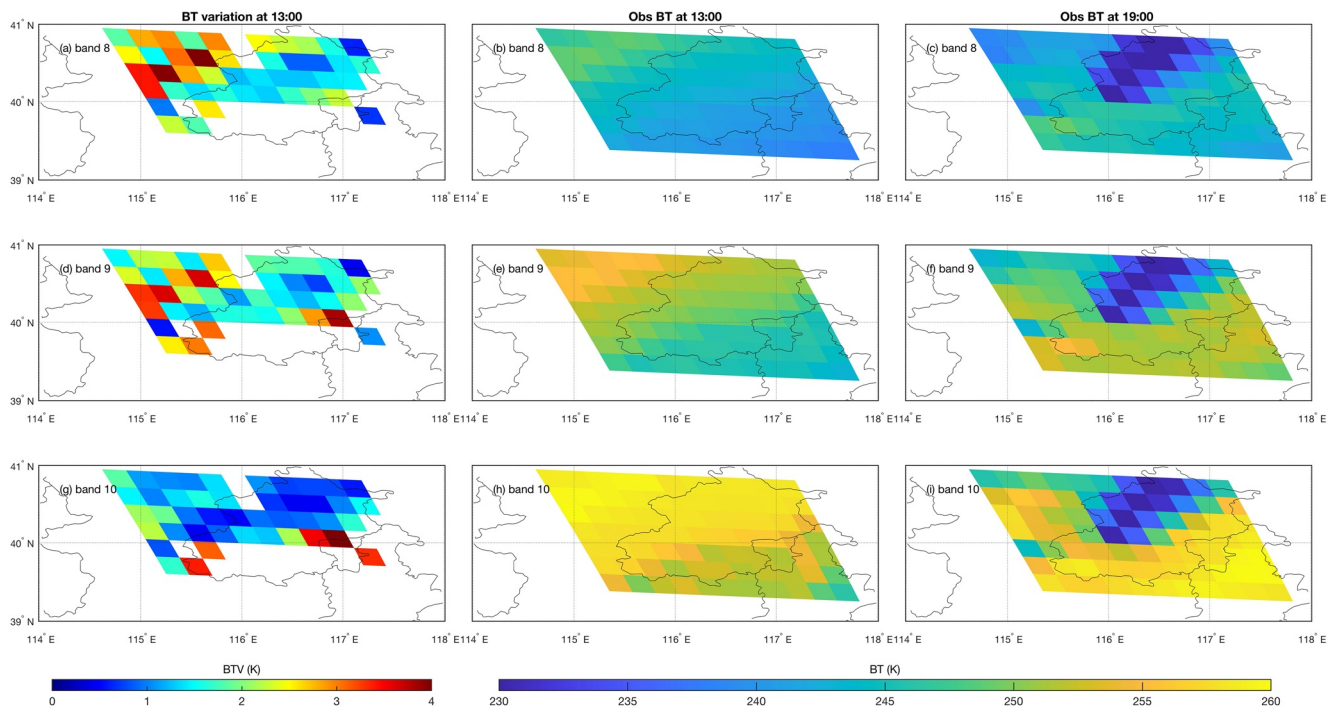
Figure 4. Clear footprint BTVs at 13:00 local time (left panels) along with the all-sky BT images (middle panels), and the all-sky BT images at 19:00 local time (right panels) for three AHI water vapor bands at July 27 of 2016.

the middle and upper troposphere. But for band 10, the BTV spatial patterns are quite different from the other two bands and the values are relatively smaller. This reflects that the atmosphere might have baroclinic instability at 13:00 local time. A strong small-scale moisture gradient is often associated with the occurrence of high-impact weather events such as cold frontlines and locally severe storms (Henken et al., 2016; Li et al., 2012). The moisture information (TPW, LPW, profile), along with atmospheric instability indices from hyperspectral IR sounder measurements in the pre-convection environment, is very useful for nowcasting and situation awareness. For example, Li et al. (2011) demonstrated that such information can help reveal local severe storm occurrence hours in advance. In this specific case, severe storms later developed as indicated by radar (not shown), as well as the BT images (right panels in Figure 4).

5. Conclusions and Discussions

AHI IR radiance measurements with high spatial resolution (2 km) are used to study the hyperspectral IR sounder sub-footprint moisture spatial variations and the coverage of clear sky and partly clear sky footprints with different spatial resolutions. It is found that:

1. The higher spatial resolution IR sounders provide more clear sky observations for data assimilation and other applications. And there is a significant increase in the annual clear footprint percentage over our study region when the spatial resolution is increased from that of the current sounders (12–16 km) to that of future sounders (4–8 km)

2. Regardless of the spatial resolution, the combined percentage of clear and partially clear footprints does not change substantially. However, through imager-based cloud-clearing processing (Li et al., 2005, 2016), radiances in partly clear footprints can be assimilated into the NWP model, which overcomes in part the limitation of coarser-resolution for data assimilation applications. Therefore, cloud-clearing is very important for applications using data from hyperspectral IR sounders, especially those with coarser resolution like GIIRS onboard FY-4A

3. The IR sounder spatial resolution impacts the sounder sub-footprint atmospheric moisture variations. It is very clear that finer spatial resolution leads to smaller sub-footprint BTVs or atmospheric moisture variations. The sub-footprint moisture variations are larger over land than over the ocean, and these

variations over land are larger in the north than in the south. The findings suggest that current hyperspectral IR sounders have limitations on capturing small-scale (e.g., storm scale) moisture variations, especially the sub-footprint moisture variations. The future GIIRS with 8 km resolution will be better able to depict moisture spatial features, and the future IRS with 4 km spatial resolution will be able to capture small-scale moisture variations. Both the GIIRS and IRS (and any other similar sensors) will also add the important temporal scale information needed for monitoring the pre-storm environments

Besides, it must be stressed that there is significant sub-footprint moisture variation over land for our current lower spatial resolution hyperspectral IR sounders, data assimilation should consider this important information, especially in the regional models. Typically the current sounders (e.g., IASI) have observation errors (radiometric and spectral calibrations, navigation, co-registration, and detector noise altogether) between 0.2 and 0.3 K for most tropospheric water vapor channels for a nominal atmosphere (Blumstein et al., 2007; Tobin et al., 2013). If the sub-footprint BTV is greater than 0.5 K, the assimilation of water vapor information will be more difficult, especially over land, which may explain why the assimilation of moisture channels over land is much more difficult than over ocean in the current operational NWP systems. Of course the surface emissivity varies much more over the land than water which could be another reason. The sub-footprint BTVs should be considered in data assimilation, especially in regional and storm scale NWP models. Quality controls to remove radiances with extremely large sub-footprint BTVs could be useful for water vapor band radiance assimilation in NWP, especially over land (J.-R. Lee et al., 2019). In addition, the sub-footprint BTVs can be useful for improving the scene-dependent observation error covariance matrix. The sub-footprint BTV should also be considered in moisture profile retrievals, especially over land, for nowcasting and situational awareness. For example, if 15% accuracy is required for profile retrievals, certain footprints with large sub-footprint BTV should be excluded in the processing or should be processed with additional information or quality control. High spatial and temporal moisture information from geostationary satellites can further add value for storm scale NWP when combined with radar observations in assimilation (Pan et al., 2021). In addition, moisture spatial variations, along with atmospheric instability indices such as the lift index and convective available potential energy from geostationary satellites are very valuable for situation awareness and nowcasting (Schmit et al., 2009, 2019). Because the spatial resolution has significant impact on applications such as nowcasting and NWP assimilation, the sub-footprint BTVs should be considered in those applications. It should be noted that some fine scale (e.g., finer than 1 km) moisture variabilities might still be missing in the analysis since the study is based on 2 km AHI pixels. Structure function analysis with aircraft Multispectral Atmospheric Mapping Sensor data (100 m resolution) showed that moisture variations typically occur at 300 m over land (Moeller et al., 1993).

This study is also relevant to the design of future advanced space-based sounding instruments, with a focus on increasing spatial resolution. It should be noted that increasing the footprint density is now very achievable using larger area format detector arrays. Maintaining measurement contiguity (i.e., a footprint spacing nearly the same as the footprint size) has been shown (Smith et al., 2009) to be important for obtaining the highest probability of sampling clear footprints for a given FOR and footprint size (Smith et al., 1996). Because large area focal plane detector arrays are now "state of the art," this technology should be considered for advancing the capability of future high spectral resolution sounders. In doing so, radiance measurements with spatial contiguity can be maintained as needed to greatly improve the clear sky sampling percentage, clear radiance measurement accuracy and yield as needed for improving NWP applications using high spectral resolution radiance data.

In summary, the IR sounder spatial resolution has a substantial impact on the clear footprint coverage and the sub-footprint moisture variation. This should be taken into account for the future planning of IR sounder observing systems and for radiance assimilation in NWP models, as well as for deriving moisture soundings for nowcasting. The current sounders have limited capability in capturing the small-scale moisture variations, while the future geostationary hyperspectral IR sounders will have much improved capability, especially the IRS onboard the MTG-S to be launched in 2023 time frame.

Data Availability Statement

The Himawari-8 AHI level 1B data, provided by Meteorological Satellite Center of the JMA, are available from the JAXA website (http://www.eorc.jaxa.jp/ptree/index.html). The views, opinions, and findings contained in this report are those of the authors and should not be construed as an official National Oceanic and Atmospheric Administration or U.S. Government position, policy, or decision.

References

Atkins, N.-T., Wakimoto, R.-M., & Ziegler, C.-L. (1998). Observations of the fine scale structure of a dryline during VORTEX 95. *Monthly Weather Review*, *126*(3), 525–555. https://doi.org/10.1175/1520-0493(1998)126<0525:ootfso>2.0.co;2

Bessho, K., Date, K., Hayashi, M., Ikeada, A., Imai, T., Inoue, H., et al. (2016). An introduction to Himawari-8/9—Japan's new-generation geostationary meteorological satellites. *Journal of the Meteorological Society of Japan*, *94*(2), 151–183. https://doi.org/10.2151/jmsj.2016-009

Blumstein, D., Tournier, B., Cayla, F.-R., Phulpin, T., Fjortoft, R., Buil, C., & Ponce, G. (2007). In-flight performance of the Infrared Atmospheric Sounding Interferometer (IASI) on METOP-A. In *Proceeding SPIE 6684*. (p. 66840H). Atmospheric and Environmental Remote Sensing Data Processing and Utilization III: Readiness for GEOSS. https://doi.org/10.1117/12.734162

Di, D., Ai, Y., Li, J., Shi, W., & Lu, N. (2016). Geostationary satellite-based 6.7 µm band best water vapor information layer analysis over the Tibetan Plateau. *Journal of Geophysical Research: Atmospheres*, *121*(9), 4600–4613. https://doi.org/10.1002/2016JD024867

Freudling, M., Egner, S., Hering, M., Carbó, F.-L., & Thiele, H. (2017). Introduction to the novel verification concept of the instrument performances for the Meteosat Third Generation InfraRed Sounder instrument (MTG-IRS). In: *International Conference on Space Optics*. https://doi.org/10.1117/12.2296097

Henken, C., Diedrich, H., Preusker, R., & Fischer, J. (2016). MERIS full-resolution total column water vapor: Observing horizontal convective rolls. *Geophysical Research Letters*, *42*(22), 10074–10081. https://doi.org/10.1002/2015GL066650

Honda, T., Miyoshi, T., Lien, G.-Y., Nishizawa, S., Yoshida, A., Adachi, S.-A., et al. (2018). Assimilating all-sky Himawari-8 satellite infrared radiances: A case of Typhoon Soudelor (2015). *Monthly Weather Review*, *146*(1), 213–229. https://doi.org/10.1175/MWR-D-16-0357.1

Iacono, M.-J., Delamere, J.-S., Mlawer, E.-J., & Clough, S.-A. (2003). Evaluation of upper tropospheric water vapor in the NCAR Community Climate Model (CCM3) using modeled and observed HIRS radiances. *Journal of Geophysical Research*, *108*(D2), 4037. https://doi.org/10.1029/2002JD002539

Kalluri, S., Alcala, C., Carr, J., Griffith, P., Lebair, W., Lindsey, D., et al. (2018). From photons to pixels: Processing data from the Advanced Baseline Imager. *Remote Sensing*, *10*(2), 177. https://doi.org/10.3390/rs10020177

King, M. D., Platnick, S., Menzel, W. P., Ackerman, S. A., & Hubanks, P. A. (2013). Spatial and temporal distribution of clouds observed by MODIS onboard the Terra and Aqua satellites. *IEEE Transactions on Geoscience and Remote Sensing*, *51*(7), 3826–3852. https://doi.org/10.1109/tgrs.2012.2227333

Lee, J.-R., Li, J., Li, Z.-L., Wang, P., & Li, J.-L. (2019). ABI water vapor radiance assimilation in a regional NWP model by accounting for the surface impact. *Earth and Space Science*, *6*, 1652–1666. https://doi.org/10.1029/2019EA000711

Lee, Y.-K., Li, J., Li, Z.-L., & Schmit, T. (2017). Atmospheric temporal variations in the pre-landfall environment of Typhoon Nangka (2015) observed by the Himawari-8 AHI. *Asia-Pacific Journal of Atmospheric Sciences*, *53*, 431–443. https://doi.org/10.1007/s13143-017-0046-z

LeMone, M.-A., Zipser, E.-J., & Trier, S.-B. (1998). The role of environmental shear and thermodynamic conditions in determining the structure and evolution of mesoscale convective systems during TOGA COARE. *Journal of the Atmospheric Sciences*, *55*(23), 3493–3518. https://doi.org/10.1175/1520-0469(1998)055<3493:troesa>2.0.co;2

Li, J., Li, J.-L., Otkin, J., Schmit, T.-J., & Liu, C. (2011). Warning information in a preconvection environment from the geostationary advanced infrared sounding system—A simulation study using IHOP case. *Journal of Applied Meteorology and Climatology*, *50*, 776–783. https://doi.org/10.1175/2010JAMC2441.1

Li, J., Liu, C.-Y., Huang, H.-L., Schmit, T.-J., Menzel, W.-P., Gurka, J., & Gurka, J. J. (2005). Optimal cloud-clearing for AIRS radiances using MODIS. *IEEE Transactions on Geoscience and Remote Sensing*, *43*, 1266–1278. https://doi.org/10.1109/TGRS.2005.847795

Li, J., Liu, C.-Y., Zhang, P., & Schmit, T.-J. (2012). Applications of full spatial resolution space-based advanced infrared soundings in the preconvection environment. *Weather and Forecasting*, *27*, 515–524. https://doi.org/10.1109/TGRS.2005.847795

Li, J., Menzel, W.-P., Sun, F., Schmit, T.-J., & Gurka, J. (2004). AIRS subpixel cloud characterization using MODIS cloud products. *Journal of Applied Meteorology and Climatology*, *43*, 10832–11094. https://doi.org/10.1175/1520-0450(2004)043<1083:asccum>2.0.co;2

Li, J., Okamoto, K., Geer, A., Otkin, J., Liu, Z., Han, W., & Wang, P. (2021). Satellite all-sky infrared radiance assimilation: Recent progress and future perspectives. *Advances in Atmospheric Sciences*. https://doi.org/10.1007/s00376-021-1088-9

Li, J., Wang, P., Han, H., Li, J., & Zheng, J. (2016). On the assimilation of satellite sounder data in cloudy skies in the numerical weather prediction models. *Journal of Meteorological Research*, *30*, 169–182. https://doi.org/10.1007/s13351-016-5114-2

Lu, J., Feng, T., Li, J., Cai, Z.-L., Xu, X.-J., Li, L., & Li, J.-L. (2019). Impact of assimilating Himawari-8 derived layered precipitable water with varying cumulus and microphysics parameterization schemes on the simulation of Typhoon Hato. *Journal of Geophysical Research: Atmospheres*, *124*(6), 3050–3071. https://doi.org/10.1029/2018JD029364

Ma, Z., Li, J., Han, W., Li, Z., Zeng, Q., Menzel, W.-P., et al. (2021). Four-dimensional wind fields from geostationary hyperspectral infrared sounder radiance measurements with high temporal resolution. *Geophysical Research Letters*, *48*(14), e2021GL093794. https://doi.org/10.1029/2021GL093794

Menzel, W.-P., Achtor, T.-H., Hayden, C.-M., & Smith, W.-L. (1984). The Advantages of Sounding with the Smaller Detectors of the VISSR Atmospheric Sounder. NOAA Technical Memorandum NESDIS 6.

Menzel, W.-P., Schmit, T.-J., Zhang, P., & Li, J. (2018). Satellite-based atmospheric infrared sounder development and applications. *Bulletin of the American Meteorological Society*, *99*(3), 583–603. https://doi.org/10.1175/BAMS-D-16-0293.1

Min, M., Wu, C.-Q., Li, C., Liu, H., Xu, N., Wu, X., et al. (2017). Developing the science product algorithm testbed for Chinese next-generation geostationary meteorological satellites: Fengyun-4 series. *Journal of Meteorological Research*, *31*(4), 708–719. https://doi.org/10.1007/s13351-017-6161-z

Moeller, C.-C., Menzel, W.-P., & Strabala, K.-I. (1993). High-resolution depiction of atmospheric moisture, stability, and surface temperature from combined MAMS and VAS radiances. *International Journal of Remote Sensing*, *14*(6), 1133–1158. https://doi.org/10.1080/01431169308904401

Nagle, F. W., & Holz, R. E. (2009). Computationally efficient methods of collocating satellite, aircraft, and ground observations. *Journal of Atmospheric and Oceanic Technology*, *26*(8), 1585–1595. https://doi.org/10.1175/2008jtecha1189.1

Pan, S., Gao, J., Jones, T.-A., Wang, Y., Wang, X., & Li, J. (2021). The impact of assimilating satellite-derived layered precipitable water, cloud water path and radar data on short-range thunderstorm forecasts. *Monthly Weather Review*, *149*(5), 1359–1380. https://doi.org/10.1175/MWR-D-20-0040.1

Schmetz, J., Stuhlmann, R., Grandell, J., Tjemkes, S., Calbet, X., Koenig, M., et al. (2012). *Meteosat Third Generation (MTG) development in the context of other future geostationary satellite observations*. American Geophysical Union.

Schmit, T.-J., Griffith, P., Gunshor, M.-M., Daniels, J.-M., Goodman, S.-J., & Lebair, W.-J. (2017). A closer look at the ABI on the GOES-R Series. *Bulletin of the American Meteorological Society*, *98*(4), 681–698. https://doi.org/10.1175/bams-d-15-00230.1

Schmit, T.-J., Gunshor, M.-M., Menzel, W.-P., Gurka, J.-J., Li, J., & Bachmeier, A.-S. (2005). Introducing the next-generation Advanced Baseline Imager on GOES-R. *Bulletin of the American Meteorological Society*, *86*(8), 1079–1096. https://doi.org/10.1175/bams-86-8-1079

Schmit, T. J., Li, J., Ackerman, S. A., & Gurka, J. J. (2009). High-spectral-and high-temporal-resolution infrared measurements from geostationary orbit. *Journal of Atmospheric and Oceanic Technology*, *26*(11), 2273–2292. https://doi.org/10.1175/2009JTECHA1248.1

Schmit, T.-J., Li, J., Su, J.-L., Li, Z., Cronce, L., Lee, Y. K., et al. (2019). Legacy atmospheric profiles and derived products from GOES-16: Validation and applications. *Earth and Space Science*, *6*(9), 1730–1748. https://doi.org/10.1029/2019EA000729

Seemann, S.-W., Li, J., Menzel, W.-P., & Gumley, L.-E. (2003). Operational retrieval of atmospheric temperature, moisture, and ozone from MODIS infrared radiances. *Journal of Applied Meteorology and Climatology*, *42*, 1072–1091. https://doi.org/10.1175/1520-0450(2003)042<1072:oroatm>2.0.co;2

Smith, W. L., Huang, H. L., & Jenney, J. A. (1996). An advanced sounder cloud contamination study. *Journal of Applied Meteorology and Climatology*, *35*, 1249–1255. https://doi.org/10.1175/1520-0450(1996)035<1249:aasccs>2.0.co;2

Smith, W. L., Revercomb, H., Bingham, G., Larar, A., Huang, H., Zhou, D., et al. (2009). Evolution, current capabilities, and future advance in satellite ultra-spectral IR sounding. *Atmospheric Chemistry and Physics*, *9*(15), 1–5574. https://doi.org/10.5194/acp-9-5563-2009

Soden, B. J., & Bretherton, F. P. (1993). Upper tropospheric relative humidity from the GOES 6.7 μm channel: Method and climatology for July 1987. *Journal of Geophysical Research: Atmospheres*, *98*(D9), 16669–16688. https://doi.org/10.1029/93JD01283

Tobin, D., Revercomb, H., Knuteson, R., Taylor, J., Best, F., Borg, L., et al. (2013). Suomi-NPP CrIS radiometric calibration uncertainty. *Journal of Geophysical Research: Atmospheres*, *118*(18), 10589–10600. https://doi.org/10.1002/jgrd.50809

Wang, F., Li, J., Schmit, T. J., & Ackerman, S. A. (2007). Trade-off studies of a hyperspectral infrared sounder on a geostationary satellite. *Applied Optics*, *46*(2), 200–209. https://doi.org/10.1364/AO.46.000200

Wang, P., Li, J., Goldberg, M. D., Schmit, T.-J., Lim, A. H. N., Li, Z., et al. (2015). Assimilation of thermodynamic information from advanced IR sounders under partially cloudy skies for regional NWP. *Journal of Geophysical Research: Atmospheres*, *120*. https://doi.org/10.1002/2014jd022976

Wang, P., Li, J., Li, J.-L., Li, Z.-L., Schmit, T.-J., & Bai, W.-G. (2014). Advanced infrared sounder subpixel cloud detection with imagers and its impact on radiance assimilation in NWP. *Geophysical Research Letters*, *41*(5), 1773–1780. https://doi.org/10.1002/2013GL059067

Wang, P., Li, J., Li, Z., Lim, A.-H.-N., Li, J.-L., Schmit, T. J., & Goldberg, M. D. (2017). The impact of Cross-track Infrared Sounder (CrIS) cloud-cleared radiances on Hurricane Joaquin (2015) and Matthew (2016) forecasts. *Journal of Geophysical Research: Atmospheres*, *122*, 201–213. https://doi.org/10.1002/2017JD027515

Wang, P., Li, J., Li, Z.-L., Lim, A.-H.-N., Li, J.-L., & Goldberg, M.-D. (2019). Impacts of observation errors on hurricane forecasts when assimilating hyperspectral infrared sounder radiances in partially cloudy skies. *Journal of Geophysical Research: Atmospheres*, *124*, 10802–10813. https://doi.org/10.1029/2019JD031029

Wang, P., Li, J., Lu, B., Schmit, T.-J., Lu, J., Yong-Keun, L., et al. (2018). Impact of moisture information from Advanced Himawari Imager measurements on heavy precipitation forecasts in a regional NWP model. *Journal of Geophysical Research: Atmospheres*, *123*(11), 6022–6038. https://doi.org/10.1029/2017JD028012

Wang, X., Min, M., Wang, F., Guo, J., Tang, S., & Tang, S. (2019). Intercomparisons of cloud mask products among Fengyun-4A, Himawari-8, and MODIS. *IEEE Transactions on Geoscience and Remote Sensing*, *57*(11), 8827–8839. https://doi.org/10.1109/TGRS.2019.2923247

Wang, Y., Liu, Z., Yang, S., Min, J., Chen, L., Chen, Y., & Zhang, T. (2018). Added value of assimilating Himawari-8 AHI water vapor radiances on analyses and forecasts for "7.19" severe storm over north China. *Journal of Geophysical Research: Atmospheres*, *123*, 3374–3394. https://doi.org/10.1002/2017JD027697

Xue, Y., Li, J., Li, Z., Lu, R., Gunshor, M. M., Moeller, S. L., et al. (2020). Assessment of upper tropospheric water vapor monthly variation in reanalyses with near-global homogenized 6.5 μm radiances from geostationary satellites. *Journal of Geophysical Research: Atmospheres*, *125*(18), e2020JD032695. https://doi.org/10.1029/2020JD032695

Yang, J., Zhang, Z., Wei, C., Lu, F., & Guo, Q. (2017). Introducing the new generation of Chinese geostationary weather satellites, Fengyun-4. *Bulletin of the American Meteorological Society*, *98*(8), 1637–1658. https://doi.org/10.1175/BAMS-D-16-0065.1

Yin, R.-Y., Han, W., Gao, Z., & Li, J. (2021). Impact of high temporal resolution FY-4A Geostationary Interferometric Infrared Sounder (GIIRS) radiance measurements on Typhoon forecasts: Maria (2018) case with GRAPES global 4D-Var assimilation system. *Geophysical Research Letters*, *48*(15). https://doi.org/10.1029/2021GL093672

Zhang, P., Li, J., Schmit, T.-J., Olso, E., Li, J.-L., & Menzel, W.-P. (2006). Impact of point spread function on infrared radiances from geostationary satellite. *IEEE Transactions on Geoscience and Remote Sensing*, *44*, 2176–2183. https://doi.org/10.1109/TGRS.2006.872096